Supporting Information

Striatal dopamine 2 receptor upregulation during development predisposes to diet-induced obesity by reducing energy output in mice

Authors and Affiliations:

Marie A. Labouesse[a,b,c,1], Andrea M. Sartori[d,e,f], Oliver Weinmann[g], Eleanor H. Simpson[a,h], Christoph Kellendonk[a,b,i], Ulrike Weber-Stadlbauer[g]

[a]Department of Psychiatry, College of Physicians and Surgeons, Columbia University, New York, NY 10032; [b]Division of Molecular Therapeutics, College of Physicians and Surgeons, Columbia University, New York, NY 10032; [c]Department of Health Sciences and Technology, ETH Zurich, 8603 Schwerzenbach, Switzerland; [d]Department of Health Sciences and Technology, ETH Zurich, 8092 Zurich, Switzerland; [e]Neuro-Urology, Spinal Cord Injury Center and Research, Balgrist University Hospital, University of Zurich, 8008 Zurich, Switzerland; [f]Brain Research Institute, University of Zurich, 8057 Zurich, Switzerland; [g]Institute of Pharmacology and Toxicology, University of Zurich-Vetsuisse, 8057 Zurich, Switzerland; [h]New York State Psychiatric Institute, New York, NY 10032; and [i]Department of Pharmacology, College of Physicians and Surgeons, Columbia University, New York, NY 10032

[1]To whom correspondence may be addressed: Marie A. Labouesse, PhD; Columbia University, New York City, NY 10032, USA; +1 (646) 774-8607; mal2307@cumc.columbia.edu

www.pnas.org/cgi/doi/10.1073/pnas.1800171115

Supplementary Figures

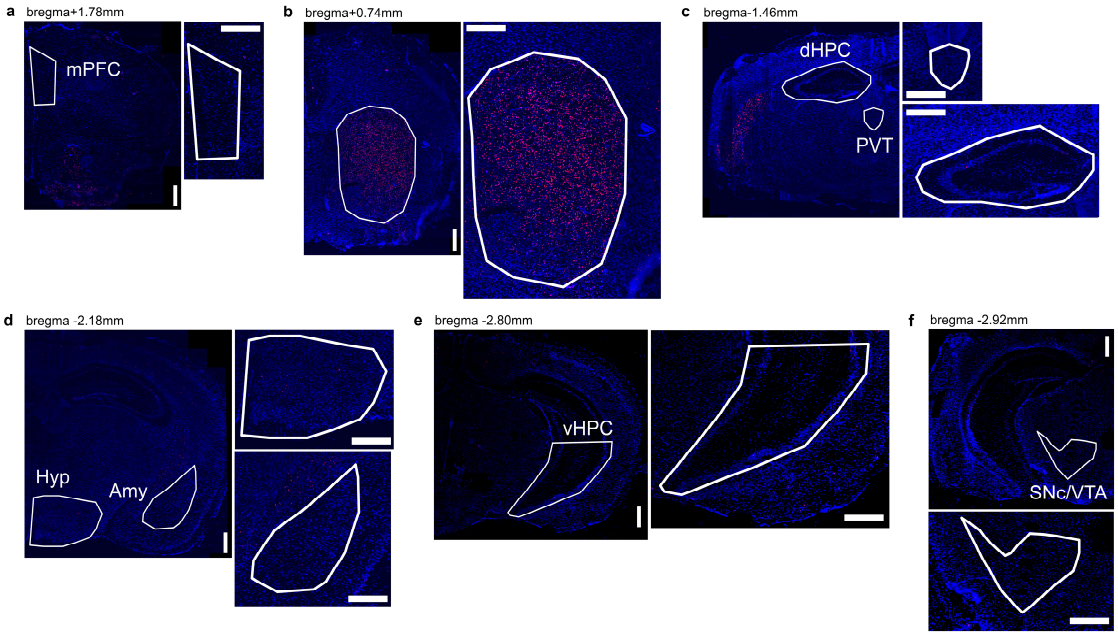

Supplementary Figure S1. Related to Figure 1. The transgene is specifically expressed in the striatum. Representative coronal brain sections of dopamine 2 receptor overexpressing mice (D2R-OE) following *in-situ* hybridization for the transgene, showing expression restricted to the striatum (including the dorsal and ventral striatum) **(b)**. There was mild or no transgene expression in other relevant brain regions (as shown in (1)). **(a)** medial prefrontal cortex (mPFC) (0.03 ± 0.03% of DAPI-positive cells), **(c)** dorsal hippocampus (dHPC) (0.52 ± 0.20% of DAPI-positive cells), paraventricular nucleus of the thalamus (PVT) (0.00 ± 0.00% of DAPI-positive cells) **(d)** hypothalamus (Hyp) (0.06 ± 0.06% of DAPI-positive cells), amygdala (Amy) (0.14 ± 0.14% of DAPI-positive cells) **(e)** ventral hippocampus (vHPC) (0.11 ± 0.01% of DAPI-positive cells) **(f)** substantia nigra compacta (SNc) and ventral tegmental area (VTA) (0.00 ± 0.00% of DAPI-positive cells). Scale bars: 500 µM. Only cells counter-stained with DAPI were counted.

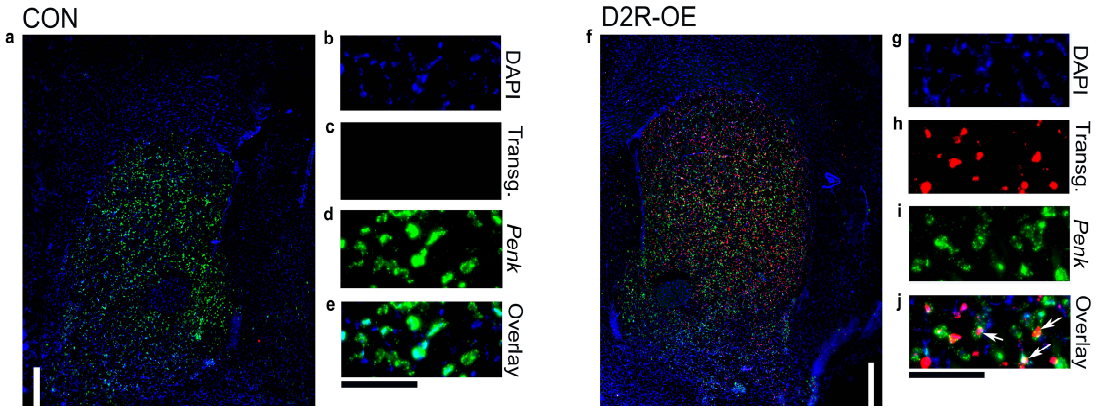

Supplementary Figure S2. Related to Figure 1. **Expression of the transgene in striatal preproenkephalin-positive (*Penk*) cells.** Representative images of fluorescent *in-situ* hybridizations for the transgene (red; **(c)** and **(h)**) and *Penk* (green; **(d)** and **(i)**) in the striatum in control (CON) **(a-e)** and dopamine 2 receptor overexpressing (D2R-OE) **(f-j)** mice. DAPI staining in blue (**(b)** and **(g)**). **(a)** and **(f):** overview of the signals in the striatal regions. 500 µM scale bar. **(b-e)** and **(g-j)**: zoom-in images showing the 3 channels when separated and when merged (**(e)** and **(j)**). 100 µM scale bar. White arrows show transgene/*Penk* double-positive cells.

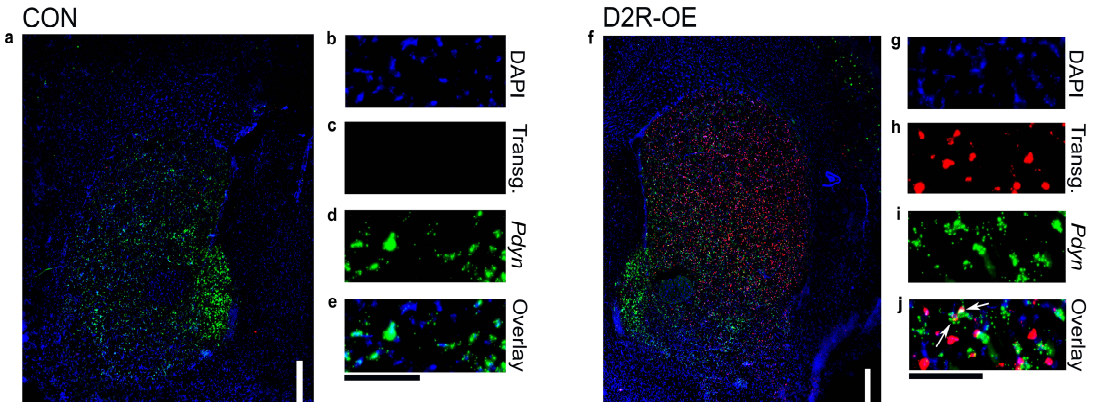

Supplementary Figure S3. Related to Figure 1. **Expression of the transgene in striatal prodynorphin-positive (*Pdyn*) cells.** Representative images of fluorescent *in-situ* hybridizations for the transgene (red; **(c)** and **(h)**) and *Pdyn* (green; **(d)** and **(i)**) in the striatum in control (CON) **(a-e)** and dopamine 2 receptor overexpressing (D2R-OE) **(f-j)** mice. DAPI staining in blue (**(b)** and **(g)**). **(a)** and **(f):** overview of the signals in the striatal regions. 500 µM scale bar. **(b-e)** and **(g-j)**: zoom-in images showing the 3 channels when separated and when merged (**(e)** and **(j)**). 100 µM scale bar. White arrows show transgene/*Pdyn* double-positive cells.

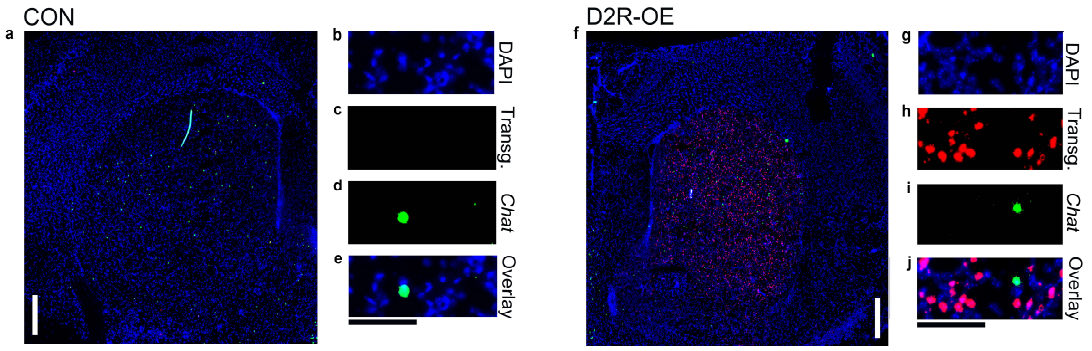

Supplementary Figure S4. Related to Figure 1. **Expression of the transgene in striatal choline acetyltransferase-positive (*Chat*) cells.** Representative images of fluorescent *in-situ* hybridizations for the transgene (red; **(c)** and **(h)**) and *Chat* (green; **(d)** and **(i)**) in the striatum in control (CON) **(a-e)** and dopamine 2 receptor overexpressing (D2R-OE) **(f-j)** mice. DAPI staining in blue (**(b)** and **(g)**). **(a)** and **(f):** overview of the signals in the striatal regions. 500 µM scale bar. **(b-e)** and **(g-j)**: zoom-in images showing the 3 channels when separated and when merged (**(e)** and **(j)**). 100 µM scale bar.

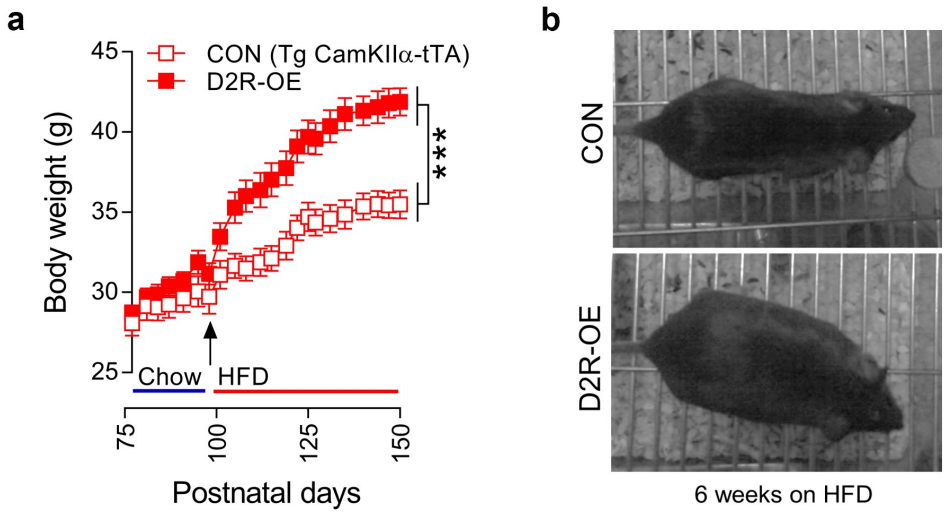

Supplementary Figure S5. Related to Figure 2. Overexpression of dopamine 2 receptors in the striatum promotes the development of obesity when fed high-fat diet (HFD).

(a) The line plot displays the absolute changes in body weight before (Chow diet; blue horizontal line) and after the start of HFD (red horizontal line) on postnatal day 98 (black arrow) in control (CON; Tg CamKIIα-tTA; see Results of **Figure 2** for explanations) and mice overexpressing D2R in the striatum (D2R-OE). ***P < 0.001 main effect of genotype. Detailed statistics in **Table S3**. All data are means±S.E.M. **(b)** Representative photographs of D2R-OE and Tg CaMKIIα-tTA controls at 6 weeks on HFD.

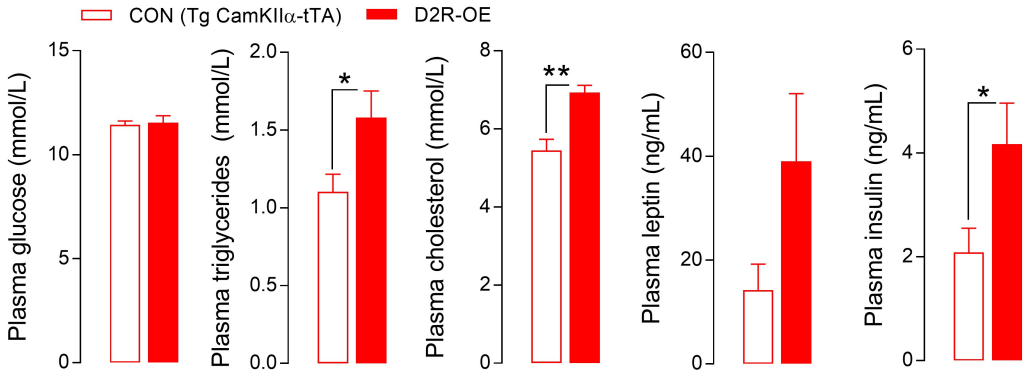

Supplementary Figure S6. Increased plasma metabolite and hormone levels in D2R-OE mice fed HFD. Related to Figure 2. D2R-OE increased fed-state plasma levels of triglycerides, cholesterol and insulin, but not glucose or leptin (at 12 weeks HFD). **P*<0.05. ***P*<0.01. Detailed statistics in **Table S3**. All data are means±S.E.M.

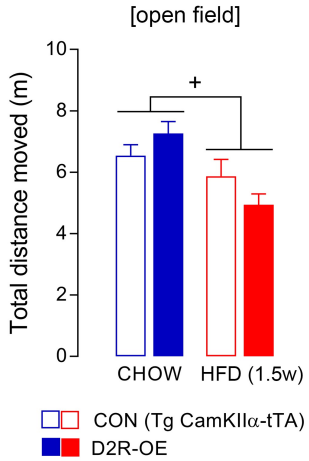

Supplementary Figure S7. Intact locomotor function in D2R-OE mice fed chow or HFD. Related to Figure 3. D2R-OE did not affect open field locomotion. $^{+}$P<0.001: main diet effect. Detailed statistics in **Table S4**. All data are means±S.E.M.

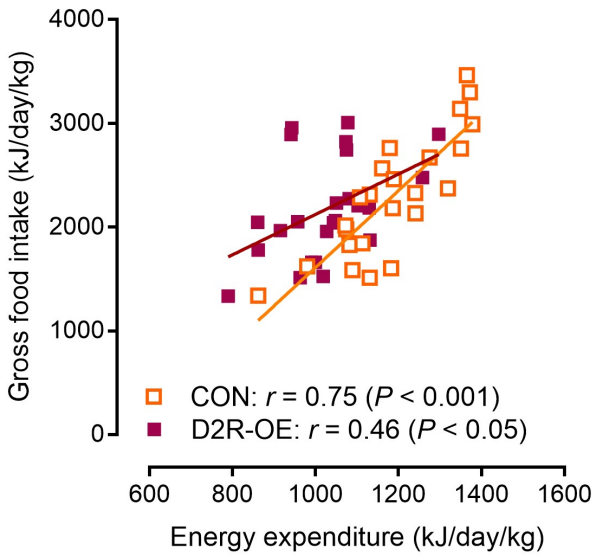

Supplementary Figure S8. Related to Figure 3. Correlation between gross food intake and energy expenditure. Statistical analyses were done using all time points (Chow, 3-day HFD, 1-week HFD, 3-weeks HFD) in **(a)** control (CON; Tg CamKIIα-tTA; n = 24 timepoints) and **(b)** mice overexpressing D2R in the striatum (D2R-OE; n=24 timepoints). Note the higher correlation coefficient (closer to 1) and stronger *P*-value in CON mice ($r = 0.75$, $P < 0.001$) as compared to D2R-OE mice ($r = 0.46$, $P < 0.05$), indicating better correlation between gross food intake and energy expenditure. N.B. Gross food intake corresponds to the total food consumed in g multiplied by the energy density of the diet in kJ/g. It corresponds to the net energy available to the body + the non-digestible component (lost through feces) + the non-metabolized energy (lost through urine and gas) (see e.g. (2)). This explains why values of gross food intake are higher than values of energy expenditure (another reason being body weight gain over time). ***P < 0.001 *P < 0.05: Pearson's product moment correlations. Detailed statistics in **Table S4**. All data are means±S.E.M.

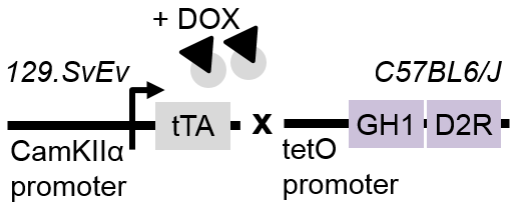

Supplementary Figure S9. Tg expression on doxycycline. Related to Figure 4. Doxycycline (DOX) binds the tetracycline transactivator tTA, precluding tTA binding to the tetracycline-operator tetO, thus shutting off the tetO-dependent transcription of the D2R transgene.

Supplementary Tables

Gene	Forward Primer	Reverse Primer
Gh1-Drd2	5‘-TGCAACATCCCGCCTGTCCTGTAC-3‘	3‘-GTGTCAAAGGCCAGCTGGTGCAGA-3‘
Pparg	5‘-AGGCGAGGGCGATCTTGACAG -3‘	3‘-AATTCGGATGGCCACCTCTTTG -3‘
Ucp1	5‘-GGGCATTCAGAGGCAAATCAGCTT-3‘	3‘-ACACTGCCACACCTCCAGTCATTA-3‘
Ppargc1a	5‘-TTC TCG ACA CAG GTC GTG TT -3‘	3‘-GTG TGC GGT GTC TGT AGT GG -3‘
Cidea	5‘-ACTTCCTCGGCTGTCTCAATGTCA -3‘	3‘-TCAGCAGATTCCTTAACACGGCCT -3‘
Adrb3	5‘-CAGCCAGCCCTGTTGAAG-3‘	3‘-CCTTCATAGCCATCAAACCTG-5‘
Rplp0	5’-GCCGTGATGCCCAGGGAAGA-3’	5’-CATCTGCTTGGAGCCCACGTT-3’

Supplementary Table 1. List of primers used in the qRT-PCR analyses. *Gh1-Drd2*: transgene vector sequence containing the human growth hormone (*Gh1*) coupled with the human dopamine 2 receptor sequence (*Drd2*); *Pparg*: peroxisome proliferator-activated receptor gamma; *Ucp1*: uncoupling protein 1; *Ppargc1a*: peroxisome proliferator-activated receptor γ coactivator 1α; *Cidea*: cell death-inducing DNA fragmentation factor alpha-like effector A; *Adrb3*: beta 3 adrenergic receptor; *Rplp0*: ribosomal protein, large, P0 (synonym: 36B4).

Assay and Figure	Dependent measures	# of mice per group	Statistical test	Effects	DF	t-Value	P-Value
%transgene positive cells (Fig. 1d, Fig S2-4)	**%transgene-+ *Penk*-+ cells** %	n(CON)= 3 n(D2R-OE)= 3	Student' *t* test with Welch corr.	Genotype	2	21.08	**<0.01**
	%transgene-+ *Pdyn*-+ cells %	n(CON)= 3 n(D2R-OE)= 3	Student' *t* test with Welch corr.	Genotype	2	8.835	**<0.05**
	%transgene-+ *Chat*-+ cells %	n(CON)= 3 n(D2R-OE)= 3	Student' *t* test with Welch corr.	Genotype	2	1	0.43

Supplementary Table S2. Summary of the statistical tests and outcomes for Figure 1 and Supplementary Figures S2-S4.

The table specifies the number of animals per test, the dependent measures for each test, the statistical test employed and the statistical outcomes. The table also specifies the corresponding degrees of freedom (DF) and F-values. Significant effects ($P < 0.05$) are given in bold font. *Chat*: choline acetyltransferase; D2R-OE: dopamine 2 receptor overexpression; *Pdyn*: prodynorphin; *Penk*: preproenkephalin

Assay and Figure	Dependent measures	# of mice per group	Statistical test	Effects	DF	F-Value	P-Value
Body weight on chow	Body weight (g)	n(WT)= 11	4 x 9 ANOVA	Genotype	(3,46)	8.74	**<0.001**
(all genotypes)		n(Tg-tetO-D2R)= 11	(Genotype x Time)	Time	(8,368)	823.69	**<0.001**
(Fig. 2b)		n(Tg-CamKII-α-tTA)=15		Genotype x Time	(24,368)	1.63	**<0.05**
		n(D2R-OE)=13					
Body weight on chow or HFD	Body weight (g)	n(WT)= 7 Chow / 4 HFD	4 x 2 ANOVA	Genotype	(3,42)	5.36	**<0.01**
(all genotypes)		n(Tg tetO-D2R)= 5 Chow / 6 HFD	(Genotype x Diet)	Diet	(1,42)	4.41	**<0.05**
(Fig. 2c)		n(Tg CaMKIIα-tTA)= 7 Chow / 8 HFD		Genotype x Diet	(3,42)	4.05	**<0.05**
		n(D2R-OE)= 6 Chow / 7 HFD					
Body composition on chow or HFD	Fat mass (g)	n(WT)= 7 Chow / 4 HFD	4 x 2 ANOVA	Genotype	(3,42)	40.03	**<0.001**
(all genotypes)		n(Tg tetO-D2R)= 5 Chow / 6 HFD	(Genotype x Diet)	Diet	(1,42)	23.11	**<0.001**
(Fig. 2d-e)		n(Tg CaMKIIα-tTA)= 7 Chow / 8 HFD		Genotype x Diet	(3,42)	5.63	**<0.001**
		n(D2R-OE)= 6 Chow / 7 HFD					
	Lean mass (g)	n(WT)= 7 Chow / 4 HFD	4 x 2 ANOVA	Genotype	(3,42)	15.21	**<0.001**
		n(Tg tetO-D2R)= 5 Chow / 6 HFD	(Genotype x Diet)	Diet	(1,42)	4.04	0.05
		n(Tg CaMKIIα-tTA)= 7 Chow / 8 HFD		Genotype x Diet	(3,42)	0.81	0.50
		n(D2R-OE)= 6 Chow / 7 HFD					
Body-weight gain on HFD	Body-weight gain (g)	n(Tg CaMKIIα-tTA)= 11	2 x 17 ANOVA	Genotype	(1,16)	10.10	**<0.01**
(Tg CaMKIIα-tTA as controls)		n(D2R-OE)= 7	(Genotype x Time)	Time	(16,256)	89.87	**<0.001**
(Fig. 2f)				Genotype x Time	(16,256)	6.47	**<0.001**
Body weight on HFD	Body weight (g)	n(Tg CaMKIIα-tTA)= 11	2 x 17 ANOVA	Genotype	(1,16)	16.77	**<0.001**
(Tg CaMKIIα-tTA as controls)		n(D2R-OE)= 7	(Genotype x Time)	Time	(16,256)	89.87	**<0.001**
(Suppl Fig. S5)				Genotype x Time	(16,256)	6.47	**<0.001**

(table follows on next page)

Assay and Figure	Dependent measures	# of mice per group	Statistical test	Effects	DF	t- or F-Value	P-Value
Oral glucose tolerance test	Glycemia	n(CON)= 10	2 x 6 ANOVA	Genotype	(1,15)	13.41	**<0.05**
(Fig. 2g)	(mM)	n(D2R-OE)= 7	(Genotype x Time)	Time	(5,75)	149.19	**<0.001**
				Genotype x Time	(5,75)	13.33	**<0.001**
Insulin sensitivity test	Glycemia	n(CON)= 11	2 x 4 ANOVA	Genotype	(1,16)	2.17	0.16
(Fig. 2h)	(%baseline)	n(D2R-OE)= 7	(Genotype x Time)	Time	(3,48)	56.84	**<0.001**
				Genotype x Time	(3,48)	2.61	0.06
Plasma metabolites	Plasma glucose	n(CON)= 6	Unpaired Student's t test	Genotype	8	-0.29	0.78
(Fig S6)	(mmol/L)	n(D2R-OE)= 4					
	Plasma triglycerides	n(CON)= 6	Unpaired Student's t test	Genotype	8	-2.44	**<0.05**
	(mmol/L)	n(D2R-OE)= 4					
	Plasma cholesterol	n(CON)= 6	Unpaired Student's t test	Genotype	8	-3.82	**<0.01**
	(mmol/L)	n(D2R-OE)= 4					
	Plasma leptin	n(CON)= 5	Unpaired Student's t test	Genotype	7	-1.94	0.09
	(ng/mL)	n(D2R-OE)= 4					
	Plasma insulin	n(CON)= 5	Unpaired Student's t test	Genotype	7	-2.39	**<0.05**
	(ng/mL)	n(D2R-OE)= 4					

Supplementary Table S3. Summary of the statistical tests and outcomes for Figure 2 and Supplementary Figure S5-S6.

The table specifies the number of animals per test, the dependent measures for each test, the statistical test employed and the statistical outcomes. The table also specifies the corresponding degrees of freedom (DF) and t-values (Student's *t* tests) or F-values (ANOVAs). Statistical values for post-hoc tests are reported directly on the respective figures and figure legends. Significant effects ($P < 0.05$) are given in bold font. CON: controls; D2R-OE: dopamine 2 receptor overexpression; HFD: high-fat diet.

Assay and Figure	Dependent measures	# of mice per group	Statistical test	Effects	DF	t-, U- or F-Value	P-Value
Food intake	Gross food intake	n(CON)= 6 at all timepoints	2 x 4 ANOVA	Genotype	(1,10)	1.89	0.20
(in metabolic cages)	(kJ/day/kg)	n(D2R-OE)= 6 at all timepoints	(Genotype x Time)	Time	(3,30)	41.36	**<0.001**
(Fig. 3a)				Genotype x Time	(3,30)	5.01	**<0.001**
Food intake on HFD	Gross food intake	n(CON)= 11 mice; 4 cages	Student' t test with Welch corr	Genotype	4.87	11.07	**<0.001**
(in home cage)	(kJ/day/kg)	n(D2R-OE)= 7 mice; 3 cages					
(Fig. 3b)							
Locomotor activity	Locomotor activity	n(CON)= 6 at all timepoints	2 x 4 ANOVA	Genotype	(1,10)	3.85	0.08
(in metabolic cages)		n(D2R-OE)= 6 at all timepoints	(Genotype x Time)	Time	(3,30)	2.87	0.05
(Fig. 3c)	(beam breaks)			Genotype x Time	(3,30)	3.32	**<0.05**
Locomotor activity	Total distance moved	n(CON)= 11 Chow / 11 HFD	2 x 4 ANOVA	Genotype	(1,16)	0.03	0.86
(in open field)	(m)	n(D2R-OE)= 7 Chow / 7 HFD	(Genotype x Diet)	Diet	(1,16)	22.32	**<0.001**
(Fig. S7)				Genotype x Diet	(1,16)	6.80	**<0.05**
Energy expenditure	Energy expenditure	n(CON)= 6 at all timepoints	2 x 4 ANOVA	Genotype	(1,10)	16.93	**<0.01**
(in metabolic cages)		n(D2R-OE)= 6 at all timepoints	(Genotype x Time)	Time	(3,30)	16.55	**<0.001**
(Fig. 3d)	(kJ/day/kg)			Genotype x Time	(3,30)	1.80	0.17
Thermal imaging	Interscapular skin temperature	n(CON)= 11 at all timepoints	2 x 4 ANOVA	Genotype	(1,16)	8.44	**<0.05**
(Fig. 3e-g)	(°C)	n(D2R-OE)= 7 at all timepoints	(Genotype x Time)	Time	(3,48)	10.62	**<0.001**
				Genotype x Time	(3,48)	0.90	0.45
	Whole body temperature	n(CON)= 11 at all timepoints	2 x 4 ANOVA	Genotype	(1,16)	4.40	0.05
	(°C)	n(D2R-OE)= 7 at all timepoints	(Genotype x Time)	Time	(3,48)	8.12	**<0.001**
				Genotype x Time	(3,48)	1.62	0.20
Gene expression	*Pparg*	n(CON)= 7	Unpaired Student's t test	Genotype	(1,11)	3.75	0.08
(Fig. 3i)	(2(-DeltaC(T)) value)	n(D2R-OE)= 6					
	Ucp1	n(CON)= 7	Unpaired Student's t test	Genotype	(1,11)	5.05	**<0.05**
	(2(-DeltaC(T)) value)	n(D2R-OE)= 6					
	Ppargc1a	n(CON)= 7	Unpaired Student's t test	Genotype	(1,11)	0.88	0.37
	(2(-DeltaC(T)) value)	n(D2R-OE)= 6					
	Cidea	n(CON)= 7	Unpaired Student's t test	Genotype	(1,11)	0.10	0.76
	(2(-DeltaC(T)) value)	n(D2R-OE)= 6					
	Adrb3	n(CON)= 7	Unpaired Student's t test	Genotype	(1,11)	2.55	0.14
	(2(-DeltaC(T)) value)	n(D2R-OE)= 6					

Assay and Figure	Dependent measures	# of mice per group	Statistical test	Correlation coefficient (= r)	P-Value
Gross food intake/Energy expenditure correlation	**Gross food intake; Energy expenditure**	n(CON)= 24	Pearson's correlation	0.75	**<0.001**
(Fig. S8)	kJ/day/kg	n(D2R-OE)= 24	Pearson's correlation	0.46	**<0.05**

Supplementary Table S4. Summary of the statistical tests and outcomes for Figure 3 and Supplementary Figures S7-S8.

The table specifies the number of animals per test, the dependent measures for each test, the statistical test employed and the statistical outcomes. The table also specifies the corresponding degrees of freedom (DF) and t-values (Student's *t* tests), U-values (Mann-Whitney test) or F-values (ANOVAs). Statistical values for post-hoc tests are reported directly on the respective figures and figure legends. Significant effects ($P < 0.05$) are given in bold font. CON: controls. D2R-OE: dopamine 2 receptor overexpression; HFD: high-fat diet.

Assay and Figure	Dependent measures	# of mice per group	Statistical test	Effects	DF	F-Value	P-Value
Food intake	Gross food intake (kJ/day/kg)	n(CON, non-DOX)= 7 mice; 4 cages	2 x 2 x 4 ANOVA	Genotype	(1,9)	21.62	**<0.01**
(Fig. 4c)		n(CON, DOX)= 10 mice; 3 cages	(Genotype x DOX-Diet x Time)	DOX-Diet	(1,9)	2.00	0.19
		n(D2R-OE, non-DOX)= 7 mice; 3 cages		Time	(3,27)	39.83	**<0.001**
		n(D2R-OE, DOX)= 7 mice; 3 cages		Genotype x DOX-Diet	(1,9)	0.03	0.88
				Genotype x Time	(3,27)	7.30	**<0.01**
				DOX-Diet x Time	(3,27)	3.91	**<0.05**
				Genotype x DOX-Diet x Time	(3,27)	1.21	0.32
Body-weight gain on HFD	Body-weight gain (g)	n(CON, non-DOX)= 9	2 x 2 x 7 ANOVA	Genotype	(1,30)	15.01	**<0.001**
(Fig. 4d)		n(CON, DOX)= 10	(Genotype x DOX-Diet x Time)	DOX-Diet	(1,30)	0.03	0.86
		n(D2R-OE, non-DOX)= 7		Time	(6,180)	136.41	**<0.001**
		n(D2R-OE, DOX)= 8		Genotype x DOX-Diet	(1,30)	0.27	0.61
				Genotype x Time	(6,180)	8.98	**<0.001**
				DOX-Diet x Time	(6,180)	1.10	0.37
				Genotype x DOX-Diet x Time	(6,180)	0.96	0.45
Body composition	Fat mass (g)	n(CON, non-DOX)= 9	2 x 2 ANOVA	Genotype	(1,30)	21.41	**<0.001**
(Fig. 4e)		n(CON, DOX)= 10	(Genotype x DOX-Diet)	DOX-Diet	(1,30)	0.00	0.99
		n(D2R-OE, non-DOX)= 7		Genotype x DOX-Diet	(1,30)	0.89	0.35
		n(D2R-OE, DOX)= 8					
	Lean mass (g)	n(CON, non-DOX)= 9	2 x 2 ANOVA	Genotype	(1,30)	28.26	**<0.001**
		n(CON, DOX)= 10	(Genotype x DOX-Diet)	DOX-Diet	(1,30)	0.00	0.99
		n(D2R-OE, non-DOX)= 7		Genotype x DOX-Diet	(1,30)	0.36	0.56
		n(D2R-OE, DOX)= 8					
Thermal imaging	Interscapular skin temperature	n(CON, non-DOX)= 9	2 x 2 ANOVA	Genotype	(1,30)	15.35	**<0.001**
(Fig. 4f)	(°C)	n(CON, DOX)= 10	(Genotype x DOX-Diet)	DOX-Diet	(1,30)	0.02	0.89
		n(D2R-OE, non-DOX)= 7		Genotype x DOX-Diet	(1,30)	0.39	0.54
		n(D2R-OE, DOX)= 8					

Supplementary Table S5. Summary of the statistical tests and outcomes for Figure 4

The table specifies the number of animals per test, the dependent measures for each test, the statistical test employed and the statistical outcomes. The table also specifies the corresponding degrees of freedom (DF) and F-values. Statistical values for post-hoc tests are reported directly on the respective figures and figure legends. Significant effects ($P < 0.05$) are given in bold font. Here diet refers to the doxycycline treatment, i.e. diet enriched with doxycycline or not enriched. CON: controls. DOX: doxycycline. D2R-OE: dopamine 2 receptor overexpression; HFD: high-fat diet.

Supplementary Material and Methods (detailed)

Animals

Transgenic mice were generated according to methods described previously (1) by crossing Tg-tetO-D2R/C57BL/6J mice with Tg-CaMKIIα-tTA/129SveV mice. Tg-TetO-D2R mice express the long form of the D2R open reading frame and have been backcrossed for over 30 generations onto the C57BL/6J background and Tg-CaMKIIα-tTA mice backcrossed for over 30 generations onto the 129SveV background. Female breeders were always Tg-tetO-D2R (C57BL/6J background) as we noticed that 1) offspring body weight were substantially higher in control mice born to Tg-CamKII-α-tTA (129SvEv background) mothers vs. control mice born to Tg-tetO-D2R (C57BL6 background) mothers and 2) breedings with Tg-CamKII-α-tTA mothers had low efficiency. We therefore used male Tg-CamKII-α-tTA breeders and female Tg-tetO-D2R breeders, to avoid differences due to maternal/paternal background and imbalanced genotypes groups resulting from the poor breeding. Double transgenic mice expressed transgenic D2Rs (D2R-OE mice). Littermates carrying a single transgene (Tg-tetO-D2R or Tg-CaMKIIα-tTA) or no transgene (WT) were used as controls in the first cohort of mice (**Figure 2b-e**). Because the Tg-CaMKIIα-tTA transgene had mild but significant effects on body composition as compared to WT, we only used Tg-CaMKIIα-tTA as controls in subsequent experiments, so as to control for the effect of the Tg-CaMKIIα-tTA transgene and avoid false positive interpretations (more conservative approach). In all metabolic/obesity experiments, breeders were exposed to time-breeding so that all offspring were of comparable age (+/- 4-days of age) as described in (3, 4). Offspring were weaned on postnatal day (PND) 21, genotyped by PCR (1) and housed by genotype by P28 allowing for food intake measurements. Animals were kept in temperature- and humidity-controlled rooms (21+/-1 °C, 55 +/- 5%) and under reversed light-dark cycle (lights off: 8 AM - 8 PM). Mice that were used for transgene expression assays in **Figures 1b-c**, **Figure 4b** were aged 3-12 months. All other mice started HFD (or chow) at P90 or P98 (=3 months) lasting until P120 or P150 (=4 or 5 months). All animals had *ad libitum* access to food and water throughout the study, unless otherwise stated. All procedures described in the present study had been previously approved by the New York State Psychiatric Institutional Animal Care and Use Committees or by the Cantonal Veterinarian's Office of Zurich. All efforts were made to minimize the number of animals used and their suffering.

Transgene expression patterns in the brain: oligo *in-situ* hybridization

Transgenic expression pattern was determined by oligo *in-situ* hybridization as in (1). Mice were killed by cervical dislocation, and the brains were dissected and rapidly frozen in mounting medium (Tissue Tek, O.C.T. Compound 4583, Sakura). Cryostat sections (20 µm) were taken, postfixed for 10 min in 4% paraformaldehyde in PBS (pH 7.4), dehydrated, and stored in 100 % ethanol at 4°C until use. The slices were hybridized to a 42 base anti-sense oligonucleotide specific to the transgenic mRNA (5'GGA CAG ATT CAG TGG ATC CAT GGT GGC GGC CGA TCC GCT TGG 3', overlaps half with the *Drd2* coding sequence and half with the vector sequence containing the human growth hormone (*Gh1*). 50 ng of oligonucleotide were labeled with 50 microCi of [α33P]dATP (Perkin Elmer) using recombinant terminal transferase (La Roche). Hybridization was performed at 42°C in a solution containing 50 % formamide (Fluka), 10 % dextran sulfate, 4 x SSC, 50 mM sodium phosphate pH 7, 10 mM sodium pyrophosphate, 5 x Denhardt's, 200 µg/ml denaturated salmon sperm DNA, 200 microg/ml poly(dA), and 107 cpm/ml oligonucletide. Slides were washed first at 60°C for 30 min and then with 1 x SSC and 0.1 SSC at room temperature for 5 min. Slides were dehydrated with ethanol and exposed to film for 2 weeks.

Transgene expression in the brain: fluorescent multiplex *in-situ* hybridization

Transgenic expression pattern was determined by fluorescent multiplex *in-situ* hybridization (RNAscope, Advanced Cell Diagnostics, CA, USA). Following rapid decapitation of adult D2R-OE and CON mice (Tg-CaMKIIα-tTA) fed HFD, brains were rapidly frozen in powdered dry ice and stored at -80°C. Coronal sections of OCT-embedded brains were cut at 20 µM at -20°C and thaw-mounted onto Super Frost Plus slides (Fisher). Slides were stored at -80°C until further processing. Fluorescent *in-situ* multiplex hybridization was performed according to the RNAscope v2.0 Fluorescent Multiple Kit User Manual for fresh frozen tissue (Advanced Cell Diagnostics, Inc., CA, USA). Briefly, sections were fixed in 4% PFA, dehydrated with increasing percentage of EtOH, and treated with pretreatment-4 protease solution (Advanced Cell Diagnostics, Inc., CA, USA). Sections were then incubated with target probes for mouse prodynorphin (*Pdyn*) to label indirect-pathway medium spiny neurons (iMSNs) (pDyn-C3, Cat No. 318771, accession number NM_010076.3, probe region 33 - 700), mouse preproenkephalin (*Penk*) to label direct-pathway MSNs (dMSNs) (pEnk-C2, Cat No. 318761, accession number NM_001002927.2, probe region 106-1332), mouse choline acetyltransferase (*Chat*) to label cholinergic neurons (ChAT-C2, Cat No. 408731, accession number NM_009891.2, probe

region 1090-1952) and a custom-made probe designed to recognize the human growth hormone sequence (*Gh1*) expressed within the transgene vector sequence using 15 ZZ hybridization pairs (hGH1-No-XMm-C1, Cat No. 539081, accession number NM_000515.4, probe region 77-828). Of note, we could not use probes for *Drd2* mRNA sequences in this experiment to recognize either the human *Drd2* gene (=transgene) or the endogenous mouse *Drd2* gene (i.e. as a potential marker for iMSNs) because there is high (91%) homology between these two genes and therefore high risk of cross-hybridization. Following probe hybridization, sections underwent a series of probe signal amplification steps followed by incubation of fluorescently labeled probes (TSA fluorophore detection kit, PerkinElmer, MA, USA) designed to target the specified channel associated with the transgene (TSA plus – Cy3), *Pdyn* (TSA plus – Cy5) and *Penk* (TSA plus - Fluorescein) as a triplex, or transgene (TSA plus – Cy3) and *Chat* (TSA plus - Fluorescein) as a duplex or transgene alone (TSA plus - Fluorescein). Slides were counterstained with DAPI, and coverslipped with fluorescent mounting medium (Mowiol, Merck, Germany). High-resolution images were obtained on a fluorescent microscope (20x, Zeiss Axio Scan.Z1, Zeiss), exported using the Zen Lite software and analysed using Fiji (ImageJ).

The percentages of *Pdyn*-, *Penk*- and *Chat*-positive cells expressing the transgene were quantified using Fiji (ImageJ) in a blind-to-cell-type fashion by counting 1) all *Pdyn*-, *Penk*- and *Chat*-positive cells and 2) all cells double-positive for the transgene and *Pdyn*, *Penk* or *Chat*. To this end, channels for the three cell types were separated to count positive cells. Only cells positive for DAPI were included. Only cells with a clear circular cell-like signal were included, or alternatively cells with at least 3 individual RNAscope puncta were included. Channels were then overlaid with the transgene channel to count double-positives. Note that the transgene (red) and DAPI (blue) when overlayed appeared in certain cases in pink. In negative control brains (CaMKIIα-tTA), only 1 in 1770 *Pdyn*-positive, 1 in 263 *Chat*-positive and no *Penk*-positive cells in the striatum were positive for the transgene, confirming probe specificity. For each brain, two sections of the striatum were included (covering ventral, dorsomedial and dorsolateral regions, across bregma levels +0.6 to 1.2 mm). To determine regions of interest (ROIs), a 1038 × 865 μm^2 two-dimensional compartment was superimposed over the structure for *Pdyn* and *Penk* counts, allowing to detect >200 positive cells of each type. Because the density of *Chat* cells is very low in the striatum (<5%), a larger 1384 × 1038 μm^2 compartment was

superimposed over the structure, allowing to detect >40 positive cells per mouse. Percent labeling was averaged for n=3 D2R-OE mice and n=3 control mice.

Given that the CaMKIIα-tTA gene is also expressed in other forebrain structures (5) relevant for energy balance (medial prefrontal cortex (mPFC), amygdala (Amy), dorsal and ventral hippocampus (dHPC, vHPC), hypothalamus (Hyp)), sections spanning the entire forebrain were also included in order to determine whether the transgene was expressed in such regions. Sections from the paraventricular nucleus of the thalamus (PVT), ventral tegmental area (VTA) and substantia nigra compacta (SNc) were also included as these regions endogenously express D2R and send projections to the dorsal or ventral striatum. Bregma levels are given in the respective figures. Transgene positive cells were counted manually in 2 sections of the relevant ROIs. Total DAPI-positive cells in each ROI was determined using the threshold analysis function and the watershed plugin in Fiji (ImageJ), thus allowing to estimate the percentage of transgene-positive cells vs. total cells in each ROI. We found percentages of expression spanning 0% to 0.52% (=dHPC) across these various brain regions (0.52% is reported as the maximal value in the main text).

Transgene expression in the pancreas and muscle: PCR

Given that the expression of CaMKII-α was previously reported in the pancreas and skeletal muscle, we verified that transgene expression was restricted to the striatum, and not to these peripheral tissues. Animals were deeply anesthetized with an overdose of ketamine-xylazine. The pancreas is a RNAase-rich tissue and therefore processed first according to established protocols (6). Skeletal muscle was dissected and immediately frozen at -80°C. Mice were then perfused transcardially with ice-cold oxygenated artificial cerebral spinal fluid for 90 sec, thus removing blood. Brains were extracted and the striatum dissected and immediately frozen at -80°C. Muscle and striatum were defrosted and homogenized into 500uL Trizol. RNA was then extracted for all tissues according to manufacturer's protocol (Trizol, Invitrogen) using chloroform phase separation and isopropanol precipitation as in (7). RNA quality was assessed using a Nanophotometer (Implen, Germany). cDNA was generated using the High Capacity cDNA Reverse transcription kit (Invitrogen). PCR was performed using Taq DNA Polymerase (Titanium; Clontech). Primers specifically aligned to the transgenic *Drd2* cDNA and exon 2 of the transgene-specific human growth hormone gene (*Gh1*) polyadenylation sequence. Amplification consisted of 5 min denaturation at 95°C followed by 36 cycles (95°C for 30 s, 63°C for 30 s and 72°C for 1 min) performed with a programmable thermocycler

(Eppendorf). PCR product was then run onto an agarose gel, and imaged using an E-Gel Imager (Life Technologies). Because the amplicon spans intron 1 of the *Gh1* gene, the amplified reverse transcribed mRNA (384 bp) can be easily distinguished from putative genomic contamination (643 bp). *Rplp0* (synonym: 36B4) was used as a control gene. Primer sequences are summarized in **Supplementary Table S1** and were purchased from Life Technologies (USA).

The same protocol was used to determine whether doxycycline (DOX) treatment shuts off transgene expression in the striatum, with the difference that RNA was extracted using the AllPrep DNA and RNA MiniKit (QIAGEN) and cDNA generated using the iScript cDNA Synthesis Kit (Bio-Rad Laboratories.

Dietary manipulations

Feeding experiments and body weight monitoring were conducted according to (3). Mice were raised on a laboratory chow (Prolab Isopro RMH3000, LabDiet; USA; 13.8% of energy from fat, 60.1% from carbohydrate, 26.1% from protein; for **Figure 1b-c**) (KLIBA 3436, 16.1 kJ/g, Kliba Nafag, Switzerland; 12.3% of energy from fat, 65.3% from carbohydrate, 22.4% from protein; for **Figures 1d-g** and **Figures 2-4**) or switched to a HFD in adulthood (Sniff D12492, 19.3 kJ/g, Ssniff, Germany; corresponds to D12492 from Research Diets, USA as in (4)) with 60.5% of energy deriving from fat, 20.5% from carbohydrate, 18.9% from protein. To regulate tetO-driven expression (**Figure 4**), mice were fed DOX-supplemented diets at 40 mg/kg (same diets as above, supplemented with 0.1% chocolate flavor to mask the bitter taste of doxycycline). To avoid neophobia, mice were exposed to DOX-Chow pellets for 2 days and then switched to DOX-Chow for a total of 1 week, followed by DOX-HFD feeding. DOX feeding therefore began 2 weeks prior to the appearance of body weight differences, a duration that we have shown is sufficient to normalize D2R protein levels in D2R-OE mice (1). Home-cage food intake was averaged from two weekly measurement time points. The data is presented per kg body weight to be consistent with the energy expenditure data. Home-cage food intake was divided by the average BW for the cage (2-3 mice per cage) recorded at the same time point. CON mice ate 2.79 ± 0.19 g per day and D2R-OE mice ate 1.91 ± 0.03 g per day of HFD on average per mouse. Note that gross food intake corresponds to the total food consumed in g multiplied by the energy density of the diet in kJ/g of dry mass (not corrected for potential changes in dry mass when the food is sitting in food hoppers). It corresponds to the net energy available to the body + the

non-digestible component (lost through feces) + the non-metabolized energy (lost through urine and gas) (see e.g. (2)).

Body composition

Body composition was assessed using a quantitative nuclear magnetic resonance (NMR) scanner (Echo MRI-100H Body Composition Analyzer, Echo Medical Systems, Houston, USA) as previously described (8). All NMR measurements were made during the dark phase. Scans were performed by placing animals into a thin-walled plastic cylinder, kept immobile by insertion of a tight fitting plunger into the cylinder (no anesthesia and no restraint necessary). The tube was then placed into the sample chamber of the instrument for the duration of the scan (approximately 20 sec). This yields estimations of fat mass (all fat molecules in the body) and lean mass (all body parts containing water, excluding fat, bone minerals, free water and hair, cartilage, etc.).

Metabolic cages

A fully automated monitoring system including an open-circuit indirect calorimetry system (Phenomaster/Calo-System, TSE Systems) was used to measure circadian ingestive behavior, O_2 consumption, and CO_2 production, as previously described (8). This system determines O_2 consumption (milliliters per kilogram per hour) and CO_2 production (milliliters per kilogram per hour) with the aid of high-speed gas sensoring units and estimates energy expenditure using V_{O2} consumed and V_{CO2} produced. Home cage spontaneous activity was obtained via an infrared photobeam-based activity monitoring system. Mice were single housed in Eurostandard II home cages (67 × 207 × 140 mm, floor area 370 cm2) with food and water made available ad libitum. Measures of daily energy intake were also obtained. CON mice ate on average the following weight of food per day: 6.06 ± 0.17 g on Chow, 4.77 ± 0.16 g on HFD (3-day time point), 3.54 ± 0.18 g (1-week time point) and 4.12 ± 0.10 g (3-weeks time point). D2R-OE mice ate on average the following weight of food per day: 5.07 ± 0,31 g on Chow, 4.86 ± 0.17 g on HFD (3-day time point), 3.81 ± 0.11 g (1-week time point) and 3.54 ± 0.22 g (3-weeks time point). The cages were enclosed in an environmental control cabinet (TSE Systems GmbH) capable of maintaining specific temperature, humidity (40% relative humidity), and illumination (60 and 0 Lux during light and dark phase, respectively) parameters. Recordings were done at thermoneutrality (at 26°C, i.e. the lower range of thermoneutrality, chosen so as to minimize the

temperature change between the home-cage environment in which obesity develops and the metabolic cage environment) following previous recommendations (9, 10). Data were collected and averaged from 2 consecutive days after an initial 2-days acclimatization period. Mice had also been acclimatized to single-caging in their home cage 1 week prior to acclimatization, once per day for 2 and up to 6 hours, every second day, so as to reduce the possible confounding effects of stress during experimentation (9).

Locomotor activity in the open field

The open field exploration test was conducted in four identical square arenas (40 × 40 cm) surrounded by walls (35 cm high) according to (3). The apparatus was made of grey Plexiglas and was located in a testing room under diffused lighting (25 lux as measured in the center of the arenas). A digital camera was mounted directly above the four arenas and images were captured using the Ethovision tracking system (Noldus Technology, Wageningen, The Netherlands). The animals were gently placed in the center of the arena and allowed to explore for 30 min. Total distance moved was analyzed as a function of 5-min bins.

Oral glucose tolerance test (oGTT)

According to previously established protocols (8), mice received an oral bolus of a 20% (wt/vol) glucose solution (2 g/kg body weight) in the middle of the dark phase (2 pm) following an overnight food-deprivation period. Blood drops for glucose measurements were taken from the tail tips at baseline and at 15, 30, 60, 90 and 120 min post-glucose. Blood glucose was measured with a blood glucose monitor (Accu-Check Aviva).

Insulin sensitivity test (IST)

According to previously established protocols (8), mice received an ip injection of insulin (0.7 mU insulin/kg body weight) at the end of the dark phase (6 pm) following a 4 h food-deprivation period. Blood sampling and glucose measurements were performed identical to the oGTT at baseline and at 15, 30 and 60 min post-insulin.

Plasma metabolite assays

All mice were killed by decapitation, and trunk blood was collected in tubes containing EDTA (Titriplex III, Merck, Germany). Plasma was separated by centrifugation (10000 rpm, 10 min, 4°C) and stored at −20 °C until future analyses. Plasma metabolites (glucose, triglycerides, cholesterol) were determined using enzymatic reaction kits (Diatools, Villmergen, Switzerland) according to the manufacturer's protocol and absorbance measurements were conducted using a spectrophotometer (Cobas Mira Auto-analyzer; Hoffman La Roche, Basel, Switzerland) (11). Circulating plasma levels of insulin and leptin were quantified using a Meso-Scale Discovery (MSD) V-Plex electrochemiluminescence metabolic assay for mice, which allows sensitive detection of insulin and leptin in mouse plasma. V-plex 96-well plates coated with primary antibodies directed against insulin and leptin were used and were treated with the corresponding detecting antibodies, which were prelabeled with SULFO-TAG™ (MSD, Rockville, Maryland, USA). The plates were read using the SECTOR PR 400 (MSD) imager and analyzed using MSD's Discovery Workbench analyzer and software package. All assays were run according to the manufacturer's instructions and to previously established protocols (8).

Surface interscapular and body temperature

Surface interscapular temperature and surface body temperature were determined using an infrared camera (FLIR E60) an established and non-invasive method to detect changes in BAT activity (12). Mice were held by the tail dorsal side up on a grid (no restraint) positioned below the infrared camera. The camera was mounted on a metal stand at a focal length of 22 cm and was used to acquire a static dorsal thermal image of the mice. Maximal surface interscapular temperature (location of the BAT) and maximal body temperature were determined with the FLIR software using 2 images per mouse. Two regions of interest (ROI) were drawn, one capturing the entire body of the mouse (body ROI) and one smaller area surrounding the interscapular region (interscapular ROI). The interscapular ROI was sized 2.1 x 1.8 cm on average, and it started at the rearward base of the ears and was centered laterally on the scapulae. The body box was sized 23.1 x 9.4 cm.

BAT histology

Animals were deeply anesthetized with an overdose of Nembutal (Abbott Laboratories) and perfused transcardially with ice-cold oxygenated ACSF (NaCl 125 mM, KCl 2.5 mM, CaCl2 2.5 mM, MgCl2 2

mM, NaHCO3 26 mM, NaH2PO4 1.25 mM, glucose 25 mM; pH 7.4) for 90 sec, thus removing blood. BAT tissue was quickly dissected and split into 2 samples, one for molecular analyses (frozen at -80°C) and one for histology, post-fixed overnight into 4% phosphate-buffered paraformaldehyde solution, dehydrated into 100% Ethanol, paraffin-embedded and kept at 4°C until further processing. BAT samples were then cut into 4 µM slices, mounted on glass slides and stained with hematoxylin-eosin for morphology according to previously established protocols (8). Images were acquired with a digital camera (Axiocam HRm; Carl Zeiss) using bright-field illumination (Zeiss Axioskop, ImagerZ2, Jena, Germany).

Gene expression in BAT

RNA analyses were conducted in line with our published protocols (7). RNA was extracted from fresh BAT samples using the RNeasy Lipid Tissue Mini Kit (QIAGEN) according to the manufacturer's protocol. mRNA levels of genes of interest were quantified by SYBR Green qRT-PCR (CFX384 real-time system, Bio-Rad Laboratories) using the SsoAdvanced Universal SYBR Green supermix (Bio-Rad Laboratories), following retrotranscription with the iScript cDNA synthesis kit (Bio-Rad Laboratories). Samples were run in 384-well formats in triplicates, and *Rplp0* (synonym: 36B4) was used as the housekeeping gene as its expression was not affected by the genetic manipulations. Thermal cycling was initiated at 95°C for 30 s, followed by 39 PCR cycles (15s at 95°C; 30 s at 60°C), and a melt-curve analysis (65-95°C, 0.5°C increments at 5 sec/step). Relative target gene expression was calculated according to the 2(-Delta Delta C(T)) method. Primer sequences are summarized in **Supplementary Table S1** and were purchased from Microsynth (Switzerland).

Statistical analyses

All data were analyzed with StatView (version 5.0) using unpaired Student's *t* test (two-tailed) (with Welch's correction if unequal variances) and parametric analysis of variance (ANOVA) followed by Fisher's least significant difference (LSD) post-hoc comparisons in the case of significant interactions. Pearson's product moment correlations were also conducted (**Fig. S8**). Full statistical results for the main statistics are provided in the **Supplementary Tables S2-S5**. For the sake of clarity (in Tables S2-S5), post-hoc statistical results are reported in the figures but not in the tables. Statistical

significance was set at $P < 0.05$. All data are means±S.E.M. Time points of all assays are reported on the respective figures and figure legends.

Supplementary References

1. Kellendonk C*, et al.* (2006) Transient and selective overexpression of dopamine D2 receptors in the striatum causes persistent abnormalities in prefrontal cortex functioning. *Neuron* 49(4):603-615.

2. Al Jothery AH*, et al.* (2014) Limits to sustained energy intake. XXII. Reproductive performance of two selected mouse lines with different thermal conductance. *J Exp Biol* 217(Pt 20):3718-3732.

3. Labouesse MA*, et al.* (2017) Hypervulnerability of the adolescent prefrontal cortex to nutritional stress via reelin deficiency. *Mol Psychiatry* 22(7):961-971.

4. Labouesse MA*, et al.* (2018) MicroRNA Expression Profiling in the Prefrontal Cortex: Putative Mechanisms for the Cognitive Effects of Adolescent High Fat Feeding. *Sci Rep* 8(1):8344.

5. Mayford M*, et al.* (1996) Control of memory formation through regulated expression of a CaMKII transgene. *Science* 274(5293):1678-1683.

6. Azevedo-Pouly AC, Elgamal OA, & Schmittgen TD (2014) RNA isolation from mouse pancreas: a ribonuclease-rich tissue. *J Vis Exp* (90):e51779.

7. Labouesse MA, Dong E, Grayson DR, Guidotti A, & Meyer U (2015) Maternal immune activation induces GAD1 and GAD2 promoter remodeling in the offspring prefrontal cortex. *Epigenetics* 10(12):1143-1155.

8. Ramachandran D*, et al.* (2017) Intestinal SIRT3 overexpression in mice improves whole body glucose homeostasis independent of body weight. *Mol Metab* 6(10):1264-1273.

9. Tschop MH*, et al.* (2011) A guide to analysis of mouse energy metabolism. *Nat Methods* 9(1):57-63.

10. Virtue S, Even P, & Vidal-Puig A (2012) Below thermoneutrality, changes in activity do not drive changes in total daily energy expenditure between groups of mice. *Cell Metab* 16(5):665-671.

11. Langhans W (1991) Hepatic and intestinal handling of metabolites during feeding in rats. *Physiol Behav* 49(6):1203-1209.

12. Crane JD, Mottillo EP, Farncombe TH, Morrison KM, & Steinberg GR (2014) A standardized infrared imaging technique that specifically detects UCP1-mediated thermogenesis in vivo. *Mol Metab* 3(4):490-494.